

Chalmers University of Technology
Department of Materials and Manufacturing Technology

Examination in Phase Transformations MMK162
Advanced Engineering Materials
14.00-18.00, 28 October 2016

Aid permitted at examination: Electronic calculator of the simple type approved by Chalmers

Solutions and answers should be well worked out and motivated to get full credit.

The question pages must be submitted together with the written answers.

In the headlines below preliminary credits are given, this might be changed during correction. Solutions will be displayed on course homepage.

Assignments	Credit
1. Phase diagrams and free energy curves	11
2. Diffusion	9
3. Interfaces and microstructure	8
4. Solidification	7
5. Diffusional transformations	9
6. Diffusionless transformations	2
7. Novel metallic materials	2
8. Solid/gas interactions	2
Sum:	50

Limits for: 3 > 45% (22.5 – 30)
 4 > 60% (30.5 – 40)
 5 > 80% (40.5 – 50)

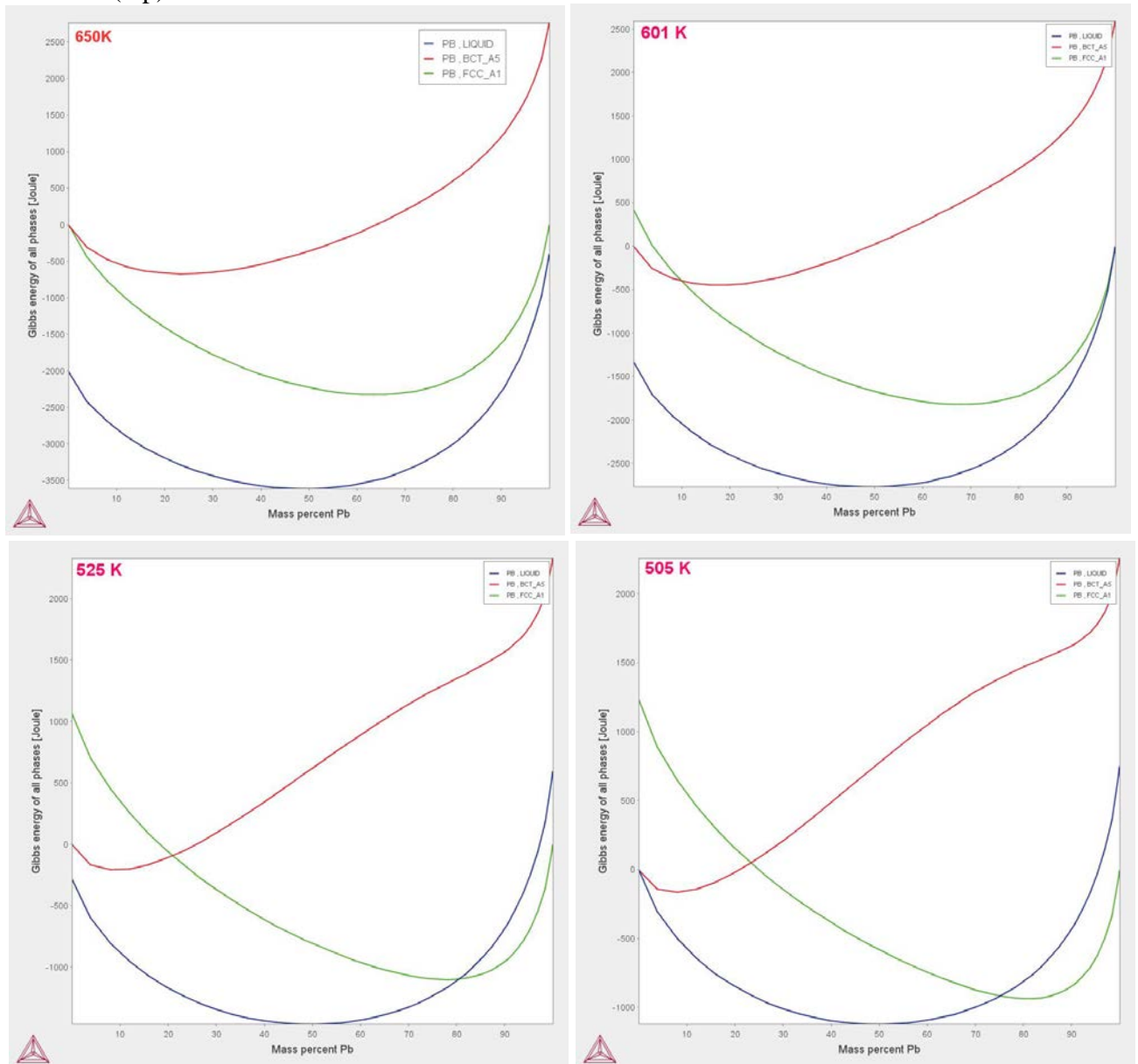
Grading will be based on the total sum of **50 points**. Bonus points earned during lectures (quiz) and individual project report will be added to the exam points.

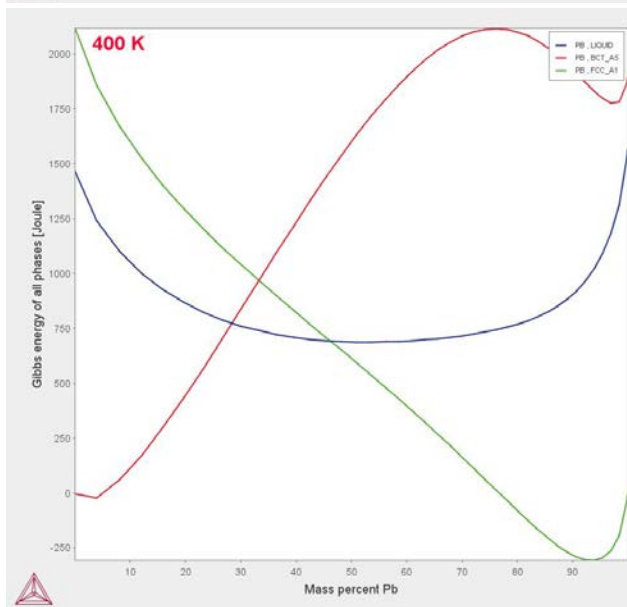
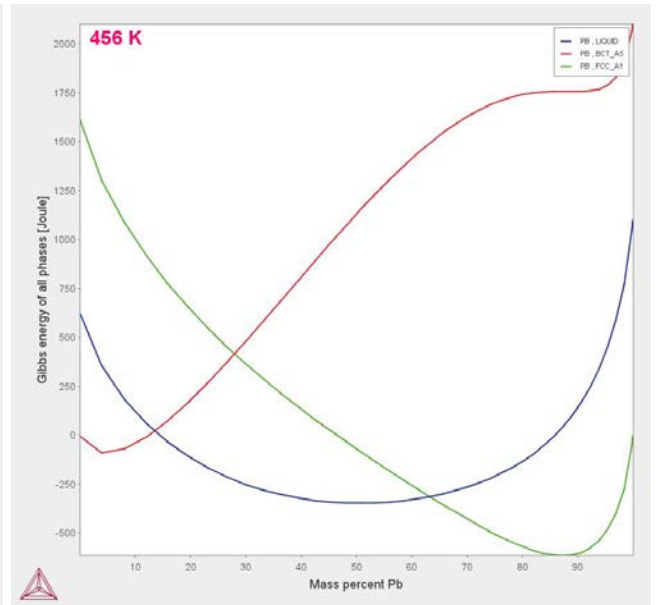
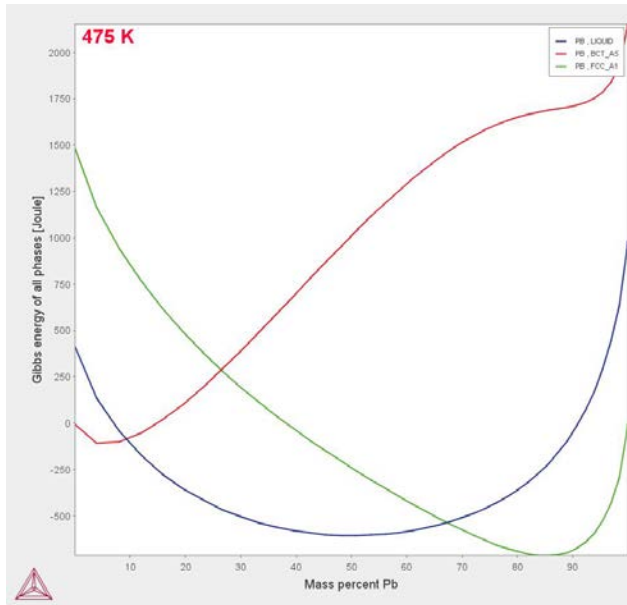
Göteborg, 2016.10.26

Assoc. Prof. Eduard Hryha

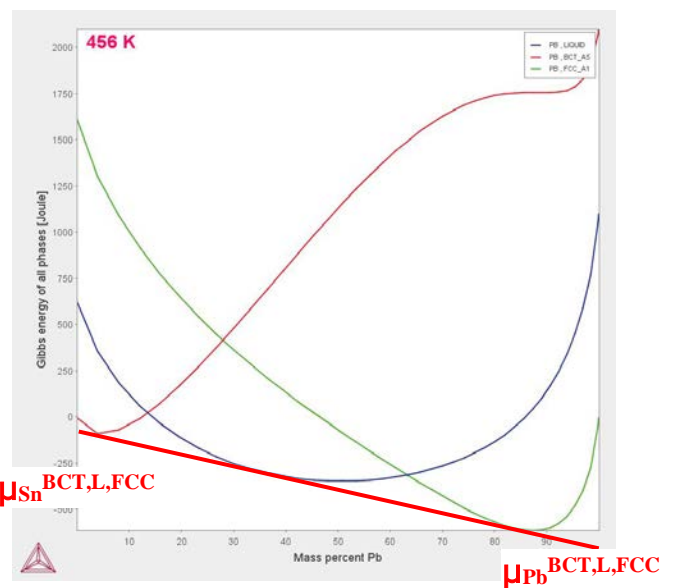
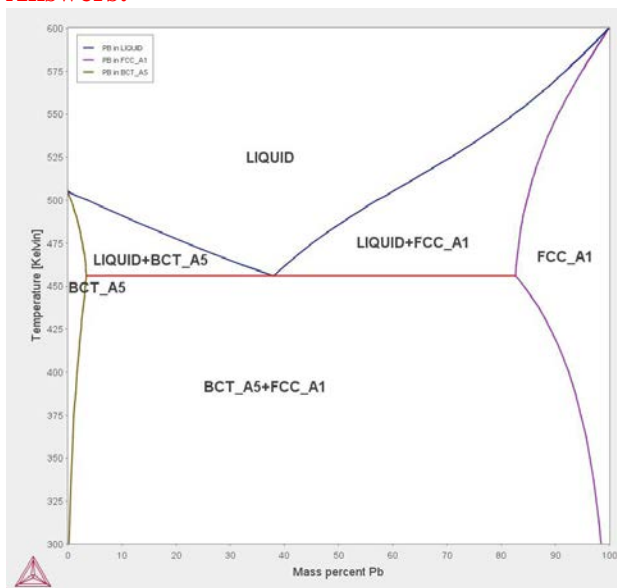
1. Phase diagrams and free energy curves (11 p)

- a) Derive phase diagram for Sn-Pb system using free energy diagrams according to the figures below. Respective temperatures are 650, 601, 525, 505, 475, 456 and 400 K (marked on the top of each figure). X and Y-axes should be drawn in correct scale compared to the phase diagram. Mark phases in the respective phase stability fields on the diagram (5).
- b) Mark chemical potentials of the phase equilibria for the free energy diagram at 456 K. (1 p)



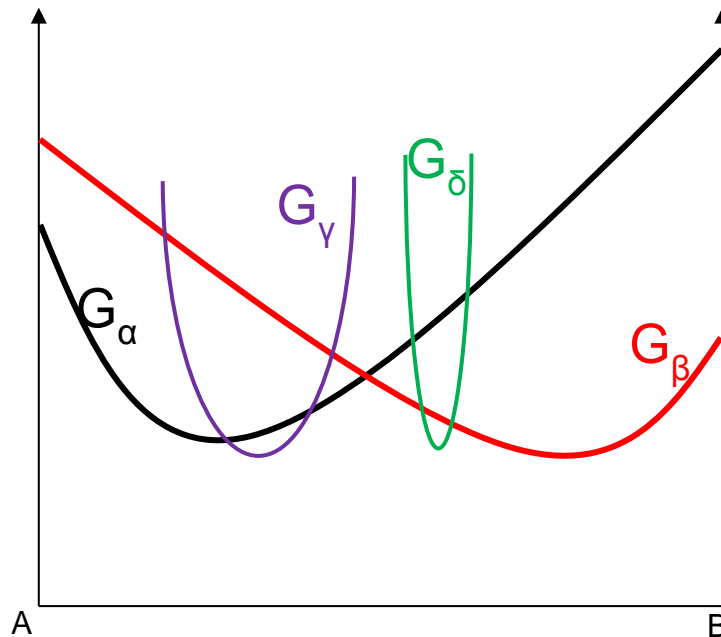


Answers:



- c) Sketch a schematic free energy diagram for a system, consisting of four phases α , β , γ and δ , where α and β has different crystal structures, γ is an intermediate phase and δ is an ordered phase. Motivation is necessary to get full credit. (2)

Answer:



- d) Describe equilibrium vacancy concentration – effect on enthalpy and entropy of the system. Plot $\Delta G = f(X_v)$ and indicate equilibrium vacancy concentration on the graph. Motivation and presentation of representative mathematical equations is necessary to get full credit. (3 p).

ANSWER:

Vacancy: broken bonds:

- increase H \rightarrow broken bonds around vacancy;
- Increase S \rightarrow increases randomness (configurational entropy)

Consider ideal/regular solution, pure metal \rightarrow only α -phase, A-A bonds stronger meaning that $\epsilon > 0$ and so $\Delta H_{mix} > 0$, X_v small:

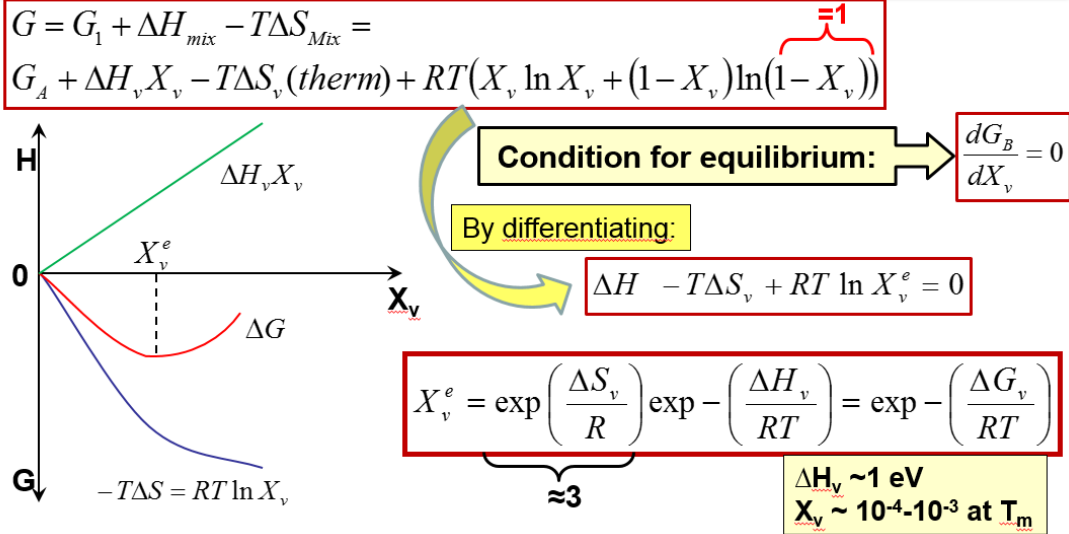
- Vacancy-vacancy interaction can be ignored so $\Delta H \approx \Delta H_v X_v$;
- $\Delta S = \Delta S_v$ (thermal) + ΔS_v (config.);
- ΔS_v (thermal) $\approx \Delta S_v X_v$ – rather small;
- ΔS_v (config.) – largest contribution:

$$\Delta S_{conf} = -R(X_v \ln X_v + (1 - X_v) \ln(1 - X_v))$$

$$\Delta S = X_v \Delta S_v (thermal) - R(X_v \ln X_v + (1 - X_v) \ln(1 - X_v))$$

See slide below for graphical representation and resulting equations:

Equilibrium Vacancy Concentration



- e)
- 2. Diffusion (9 p)**
- a) Calculate and sketch concentration profile of carbon after annealing of the weld of two steel block consisting of steels A with 0,8%C and steel B with 0,2%C. Effect of other alloying elements can be ignored. Annealing is performed at 1000°C for 30 min. Diffusion coefficient of carbon in austenite is $D=4 \cdot 10^{-11} \text{ m}^2\text{s}^{-1}$. Calculate values of the carbon content for as minimum 4 depths on each side and based on it sketch approximate graph of carbon profile. (5p).

Table 5.3 Table of the error function

z	$\text{erf } z$	z	$\text{erf } z$	z	$\text{erf } z$	z	$\text{erf } z$
0	0	0.40	0.4284	0.85	0.7707	1.6	0.9763
0.025	0.0282	0.45	0.4755	0.90	0.7970	1.7	0.9838
0.05	0.0564	0.50	0.5205	0.95	0.8209	1.8	0.9891
0.10	0.1125	0.55	0.5633	1.0	0.8427	1.9	0.9928
0.15	0.1680	0.60	0.6039	1.1	0.8802	2.0	0.9953
0.20	0.2227	0.65	0.6420	1.2	0.9103	2.2	0.9981
0.25	0.2763	0.70	0.6778	1.3	0.9340	2.4	0.9993
0.30	0.3286	0.75	0.7112	1.4	0.9523	2.6	0.9998
0.35	0.3794	0.80	0.7421	1.5	0.9661	2.8	0.9999

ANSWER:

Carbon profile in case of annealing of the joint (weld) can be described by:

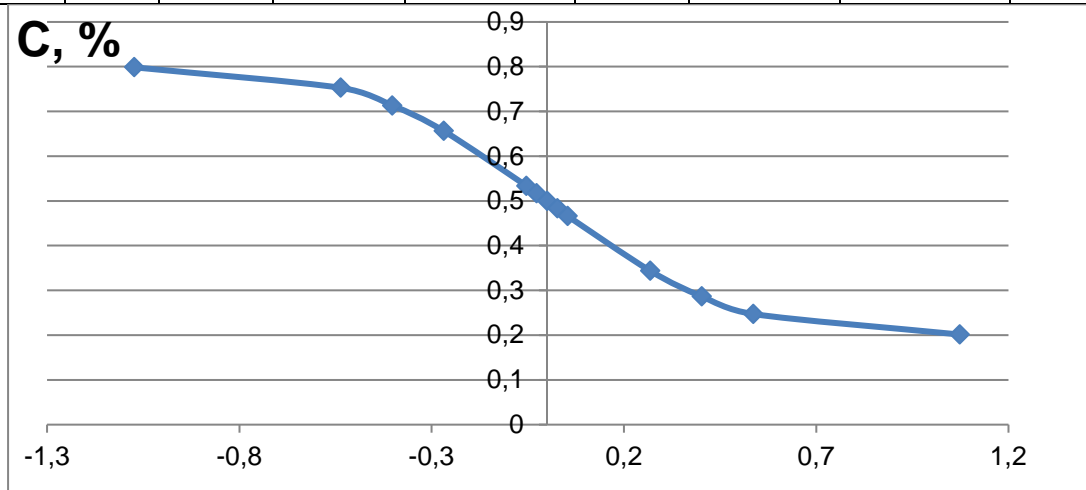
$$C = \left(\frac{C_1 + C_2}{2}\right) - \left(\frac{C_1 - C_2}{2}\right) \text{erf} \frac{x}{2\sqrt{Dt}}$$

where C_1 is carbon content in block A (0.8%C) and C_2 is

carbon content in block B (0,2%C). To simplify calculations it is easier to choose values of z and respective values of $\text{erf}(z)$ from table of values of error function. Then, by knowing the value of z and Dt you can calculate depth x . By knowing the value of $\text{erf}(z)$ you can calculate C . As $x=0$ on the weld interface, calculations has to be performed for the same/similar distances in both directions from $x=0$, considering that $\text{erf}(-z) = -\text{erf}(z)$.

The sketch of carbon profile is presented below the table.

C₁	C₂	z	erf	D	t, s	Dt	2sqrt(Dt)	C	x (mm)
0,8	0,2	-2	-0,9953	4,00E-11	1800	7,2E-08	0,000537	0,79859	-1,07331
0,8	0,2	-1	-0,8427	4,00E-11	1800	7,2E-08	0,000537	0,75281	-0,53666
0,8	0,2	-0,75	-0,7112	4,00E-11	1800	7,2E-08	0,000537	0,71336	-0,40249
0,8	0,2	-0,5	-0,5205	4,00E-11	1800	7,2E-08	0,000537	0,65615	-0,26833
0,8	0,2	-0,1	-0,1125	4,00E-11	1800	7,2E-08	0,000537	0,53375	-0,05367
0,8	0,2	-0,05	-0,0564	4,00E-11	1800	7,2E-08	0,000537	0,51692	-0,02683
0,8	0,2	0	0	4,00E-11	1800	7,2E-08	0,000537	0,5	0
0,8	0,2	0,05	0,0564	4,00E-11	1800	7,2E-08	0,000537	0,48308	0,026833
0,8	0,2	0,1	0,1125	4,00E-11	1800	7,2E-08	0,000537	0,46625	0,053666
0,8	0,2	0,5	0,5205	4,00E-11	1800	7,2E-08	0,000537	0,34385	0,268328
0,8	0,2	0,75	0,7112	4,00E-11	1800	7,2E-08	0,000537	0,28664	0,402492
0,8	0,2	1	0,8427	4,00E-11	1800	7,2E-08	0,000537	0,24719	0,536656
0,8	0,2	2	0,9953	4,00E-11	1800	7,2E-08	0,000537	0,20141	1,073313



b) Describe vacancy diffusion and relationship to the self-diffusion. Motivation and presentation of relevant equations is required to obtain full credit. (2 p)

ANSWER: see slide below

Vacancy diffusion

- equally considered as self diffusion but no need for creating a vacancy →
- omit X_v (ΔG_v) in the equation for D:

$$D_v \equiv \frac{1}{6} \Gamma_v \alpha^2$$

Equation for substitutional selfdiffusion:

$$D_A = \frac{1}{6} \alpha^2 z v \exp\left(\frac{\Delta S_m}{R}\right) \exp\left(-\frac{\Delta H_m}{RT}\right)$$

Equation for vacancy diffusion:

$$D_v = \frac{1}{6} \alpha^2 z v \exp\left(\frac{\Delta S_m}{R}\right) \exp\left(-\frac{\Delta H_m}{RT}\right)$$

$$D_0$$

$$Q_v = \Delta H_m$$

Diffusivity of vacancies is orders of magnitude greater than for substitutional atoms

$$D_v = D_A / X_v^e$$

$$D_v \gg \gg D_A$$

- c) Reaction of a cobalt nano-particles (blue) with sulfur (Co:S ratio = 9:8), see Fig.2, leads to formation of a hollow nanospheres formed by Co_9S_8 compound at the surface (yellow). Based on the figure provided, indicating different stages of formation of the nanospheres, and description provided, describe physical phenomena behind formation of such hollow nano-spheres. (2 p)

ANSWER: the reason behind formation of the hollow nanospheres is a fundamental solid-state phenomenon called Kirkendall effect. It leads directly to the formation of regular hollow nanospheres when high-quality single-crystal nanoparticles are used. The rate of diffusion of the cobalt ions toward the exterior of the nanoparticle is faster than that of the sulfur diffusing into the cobalt, and so a shell of cobalt sulfide is formed. As the cobalt nanoparticle shrinks in size, actual bridges between the cobalt core and the resulting shell are visible by transmission electron microscopy. The reaction is complete when all the cobalt is consumed and an empty pore remains inside the cobalt sulfide shell.

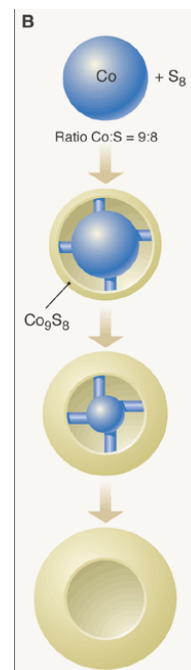


Fig.2. Formation of the Co_9S_8 nanoparticles. (J. M. Buriak, Science, 2004, 304, 692–693)

3. Interfaces and microstructure (8 p)

- a) Describe solid/vapour interfaces, namely energy of the interface, its dependence on the angle to the close-packed plane and based on it equilibrium shape of the crystal (Wulff construction). Motivation, presentation of relevant equations and graphs is required to obtain full credit. (3 p)

ANSWER: See slides below:

Solid/Vapour Interfaces

From definition of Gibbs energy, surface energy is given by:

$$\gamma_{sv} = E + PV - TS$$

- PV-ignored;
- surface atoms has higher entropy:
- thermal \rightarrow higher freedom of movement;
- configurational \rightarrow e.g. surface vacancies:

$$\gamma_{sv} \approx E - T(S_{thermal} + S_{config})$$

Experimental results: close to T_m : $\gamma_{sv_exp} = 0.15 \frac{L_s}{N_a}$

Due to entropy, γ slightly depends on T : $\left(\frac{\partial \gamma_{sv}}{\partial T}\right)_P = -S$

Surface free energy $\gamma(T_m)$ for different crystals: metals with higher T_m have high values of L_s and high surface energy

Source: M. Knutson-Wedel

Solid/Vapour Interfaces

Macroscopic surface plane: high or irrational {hkl} index

Number of broken bonds per unit area from atoms on the steps: $\frac{\sin \theta}{a} \left(\frac{1}{a}\right)$

Energy per broken bond = $\epsilon/2$:

$$E_{sv} = \frac{\cos \theta + \sin \theta}{a^2} \left(\frac{\epsilon}{2}\right)$$

Number of broken bonds per unit area parallel to steps: $\frac{\cos \theta}{a} \left(\frac{1}{a}\right)$

- Closed-packed orientation ($\theta=0$) – crisp minimum in the energy plot;
- Similar plot for $\gamma=f(\theta)$ but minimums are less prominent (entropy effect)

Solid/Vapour Interfaces

Convenient method to plot $\gamma=f(\theta) \rightarrow$ construct surface about an origin where free energy of any plane is equal to the distance between the surface and origin, measured along the normal to the plane – **Wulff construction**

Total surface energy of crystal

$$A = A_1 \gamma_1 + A_2 \gamma_2 + \dots = \sum A_i \gamma_i$$

Equilibrium shape: **Wulff construction** \rightarrow minimal surface energy $\rightarrow \sum A_i \gamma_i = \text{minimum}$

- b) Explain kinetics of the grain growth, namely: driving force, normal and abnormal grain growth, effect of secondary particles on the grain growth and factors influencing stabilization of the fine-grained structure. Presentation of the relevant equations, schematics representation of the effect of secondary particles on moving boundary and average grain size as well as motivation of the answer are necessary to get full credit. (4 p).

ANSWER:

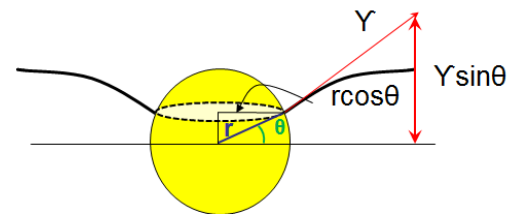
At sufficiently high temperature ($T > 0.5 T_m$) GB will migrate in order to reduce G . Rate at which mean grain diameter \bar{D} increase depends on GB mobility and driving force for migration. Assuming that mean radius of curvature r is proportional to $\bar{D} \rightarrow$ mean driving force is

proportional to $\frac{2\gamma}{\bar{D}}$: $\frac{\Delta G}{V_m} = F = \frac{2\gamma}{r}$ and hence velocity of GB migration: $v = \alpha M \frac{2\gamma}{\bar{D}} \cong \frac{d\bar{D}}{dt}$

Integration taking $\bar{D} = D_0$ when $t=0$ gives: $\bar{D}^2 = \bar{D}_0^2 + 4\alpha M \gamma \cdot t$. Experimentally found that grain growth in pure metals follows: $\bar{D} = K't^n$ where $n \approx 0.5$ only for very pure metals or at very high temperatures, otherwise $n \ll 0.5$.

Description of the thermally activated grain growth, presented above, is valid for **normal** grain growth. **Abnormal** grain growth \rightarrow growth of just a few grains to very large diameters (discontinuous grain growth, coarsening or secondary recrystallization) – happens when normal grain growth ceases due to the presence of fine particulate array.

In case of presence of secondary particles on grain boundaries, GB is attached to the particle along a length $2\pi r \cos \theta$ and so particle exert pulling force $P = \pi r \gamma$ when $\sin \theta \cos \theta \rightarrow \max$ ($\theta = 45^\circ$).

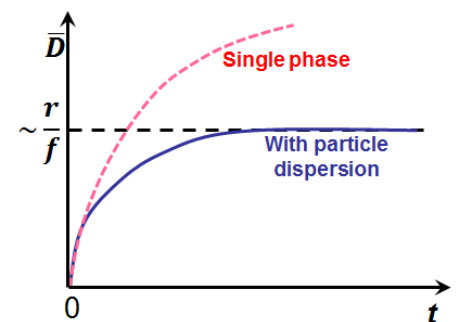


Restraining force on boundary by particle drag oppose driving force for the grain growth ($\sim \frac{2\gamma}{\bar{D}}$) is $\frac{2\gamma}{\bar{D}} = \frac{3f\gamma}{2r}$

(where f is the volume fraction of particles with radius r).

Hence, maximum grain size can be evaluated as $\bar{D}_{\max} = \frac{4r}{3f}$.

Stabilization of fine grain size requires large volume fraction of very small particles: $\bar{D}_{\max} = \frac{4r}{3f}$. If temperature is too high particles tend to coarsen or dissolve and as a result abnormal grain growth can occur.



- c) Describe mobility of the different types of grain boundaries and effect of the segregation on them. Describe effect of the temperature and solubility on segregation. Presentation of the relevant equations as well as motivation of the answer are necessary to get full credit. (1 p).

ANSWER

- Random high angle boundary – open, high mobility
- Special high angle boundary – low mobility but can have higher mobility than random. The reason for this is that impurities stick to random high angle boundaries and so decrease their mobility.

- Decreased solid solubility in the matrix: further lowered mobility due to increased grain

$$X_b \cong X_0 \exp \frac{\Delta G_b}{RT}$$

boundary concentration, X_b

Free energy released when a solute atom is moved from the matrix to the grain boundary, ΔG_b :

- ΔG_b is usually positive and increases with increasing of misfit between the solute and the matrix;
- Grain boundary segregation decreases as temperature increases – “evaporation” of the solute into the matrix;
- For low temperatures and high $\Delta G_b \rightarrow X_b$ approaches unity – maximum saturation value;
- Boundary mobility varies markedly between elements – segregation increases as the matrix solubility decreases;
- Solute atoms exert drag on the boundary that reduces boundary velocity;
- ΔG_b measures tendency of segregation.

4. Solidification (7 p)

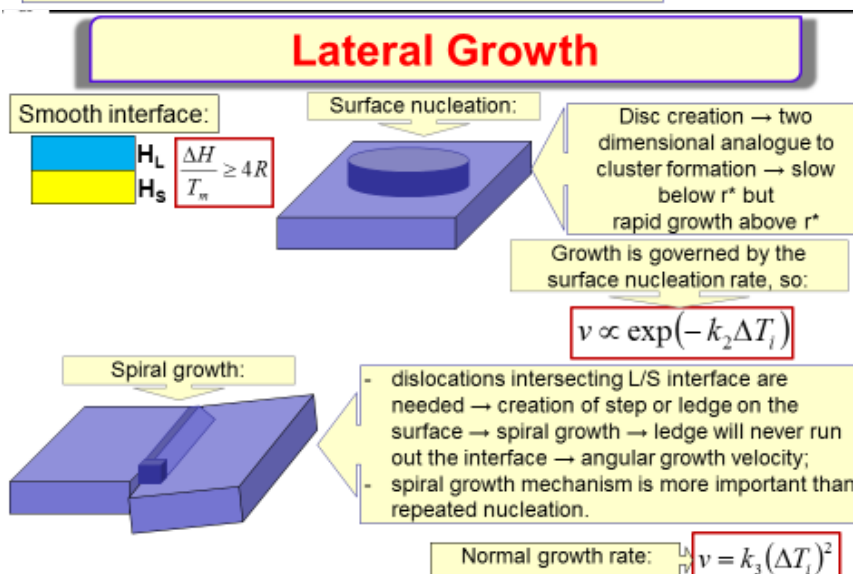
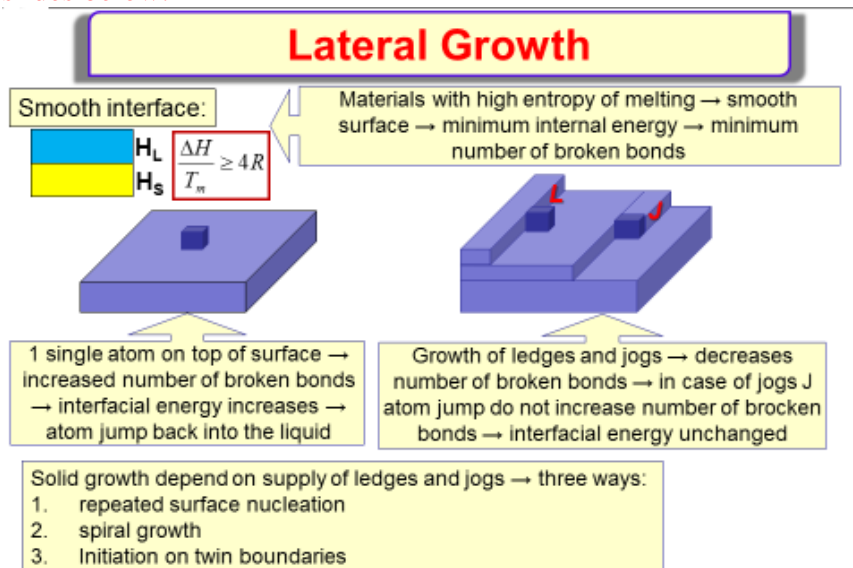
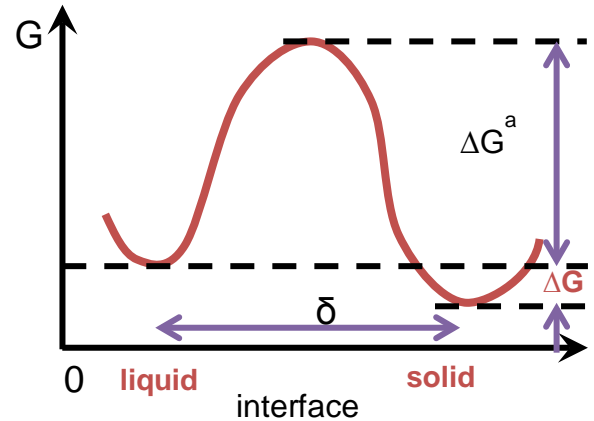
a) Describe the properties and growth mechanism of solid characterised by atomically smooth interfaces. Describe possible mechanisms of growth of smooth interfaces during solidification and their growth kinetic. Schematic presentation of the different growth mechanisms and relevant equations are necessary to get full credit. (3 p).

ANSWER

- Atomically smooth interfaces are characterised by the high energy of the interface $\frac{\Delta H}{T_m} \geq 4R$ - transition over narrow transition zone ~ 1 atomic layer and though migrate by lateral growth: Driving force for solidification

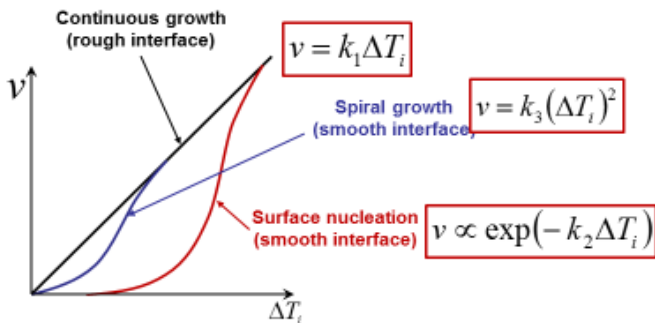
$$\Delta G = \frac{L}{T_m} \Delta T_i$$

Growth by ledge mechanism, growth kinetics is determined by supply of ledges and jogs, see slides below:



Lateral Growth

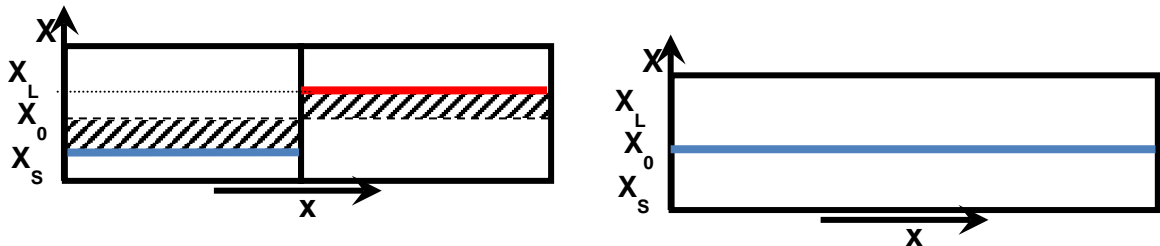
Growth from twin intersections: two crystals in different orientation are in contact → twin boundary → act as permanent source of new "steps"



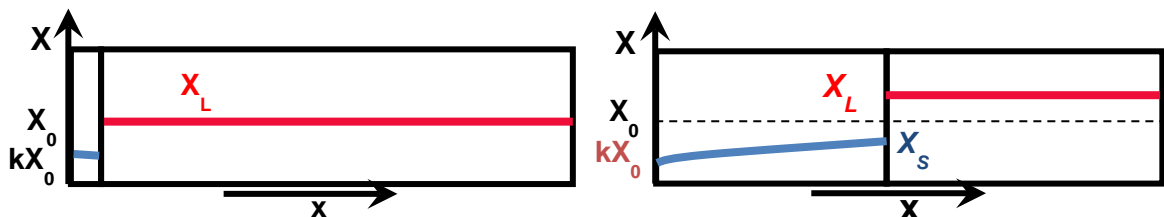
b) Shortly describe three cases of the unidirectional solidification in solid bar (Case 1 – case 3). Sketch respective concentration profile of the solute along the solidifying bar and concentration profile in the liquid in front of the solidifying interface during different stages of the solidification as well as in the fully solidified bar. Presentation of the relevant equations, sketch of the concentration profiles as well as motivation of the answer are necessary to get full credit. (4 p).

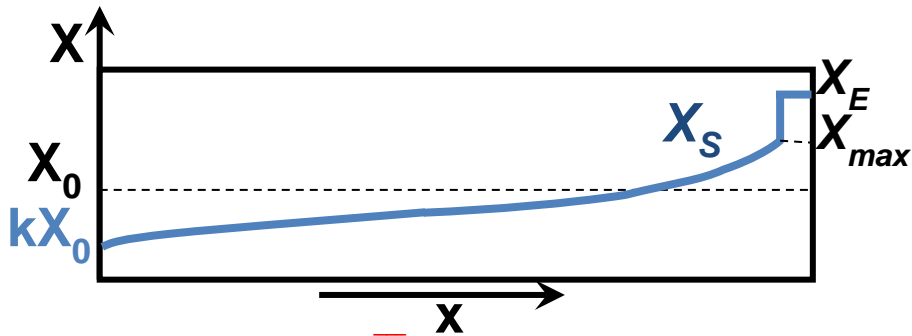
ANSWER:

- **Case 1:** Infinitely slow (equilibrium) solidification - alloy X_0 starts to solidify at T_1 with composition kX_0 . As temperature is lowered → provided cooling is slow enough to allow extensive solid state diffusion → solid and liquid are always homogeneous in composition and follows solidus and liquidus lines. Concentration profiles during solidification and in the solidified bar:



- **Case 2:** No diffusion in solid/perfect mixing in liquid. Liquid is kept homogeneous by efficient stirring. First solid will appear when T_1 is reached. Since $kX_0 < X_0$ → solute is rejected in the liquid → liquid become progressively richer in solute. Concentration profiles during solidification and in the solidified bar:





Mean composition of the solid \bar{X}_S is always lower than the composition at solid/liquid interface. Variation of X_S along solidified bar can be obtained by equating solute rejected into the liquid when small amount of solid forms with the resulting solute increase in the liquid – Scheil equations:

$$(X_L - X_S)df_s = (1 - f_s)dX_L$$

$f_s \rightarrow$ volume fraction solidified

Integrating using boundary conditions $X_S = kX_0$ when $f_s = 0$ gives:

$$X_S = kX_0(1 - f_s)^{(k-1)}$$

$$X_L = X_0 f_L^{(k-1)}$$

Case 3: No Diffusion in Solid, Diffusional Mixing in Liquid

This mechanism is observed when there is no stirring or convection in liquid. In this case solute rejected from the liquid transported away only by diffusion and hence results in rapid build-up of solute ahead of the solid. Steady state is reached at T_3 when liquid adjacent to solid has composition X_0/k and solid forms with the bulk composition $X_0 \rightarrow$ solute diffuses down the concentration gradient in liquid at the same rate as its rejected from the solid:

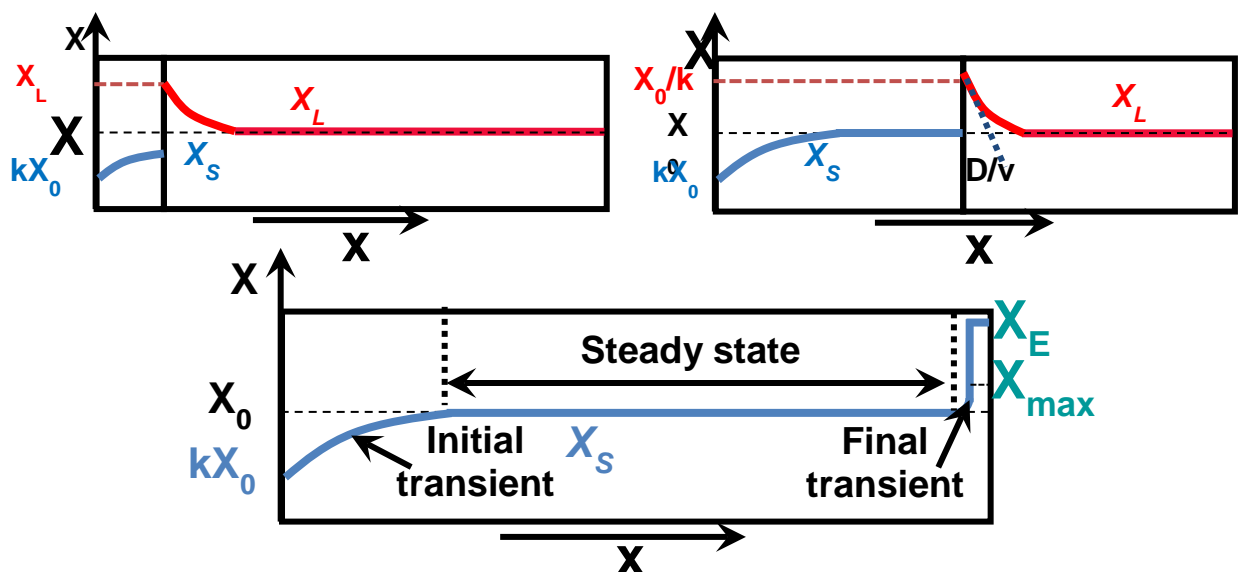
$$-DC'_L = v(C_L - C_S)$$

Solution for steady-state solidification:

$$X_L = X_0 \left\{ 1 + \frac{1-k}{k} \exp \left[-\frac{x}{(D/v)} \right] \right\}$$

Concentration profile in liquid has characteristic width D/v .

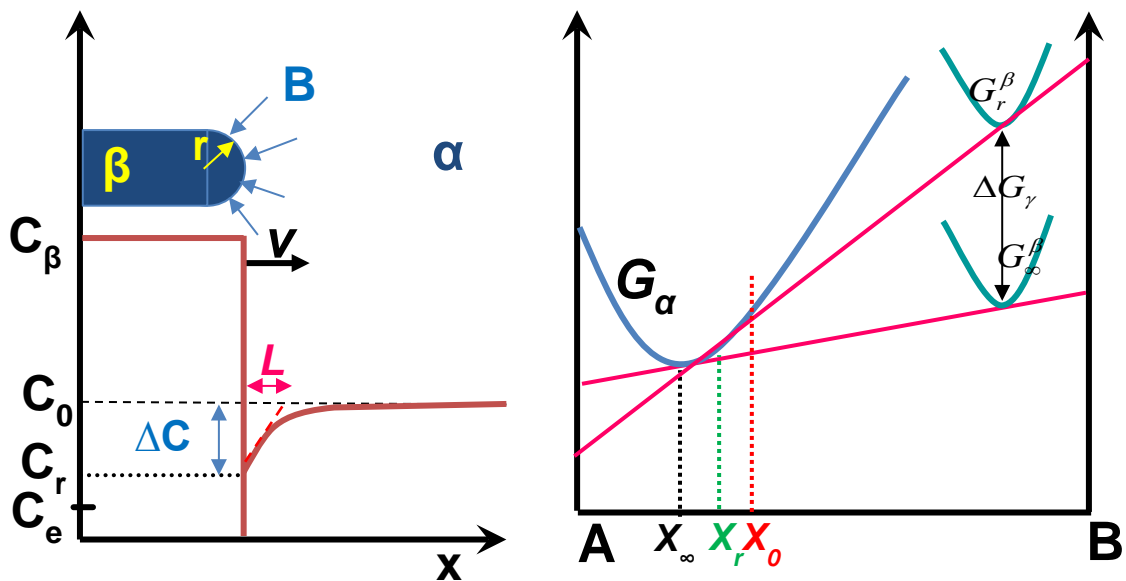
Concentration profiles during solidification and in the solidified bar:



5. Diffusional transformations (9 p).

a) Describe diffusion-controlled lengthening of plates or needles for precipitate with the constant thickness and incoherent curved edge. Sketch concentration profiles ahead of precipitation front and describe driving force for diffusion. Presentation of the relevant equations and sketch of the Gibbs free energy diagram as well as motivation of the answer are necessary to get full credit. (3 p).

ANSWER: For the precipitate with constant thickness and cylindrically curved incoherent edge it is important to take into account effect of the surface curvature – Gibbs-Thomson effect – on solubility of the solute in the matrix: due to Gibbs-Thomson effect ($G_r > G_\infty$) solubility of B-atoms in matrix is increased to C_r . This means that concentration gradient, providing driving force for diffusion, also **decrease**: $\Delta C = C_0 - C_r$. Solution shows that $L = kr$ where $k = \text{const} (\sim 1)$.



Compositional difference driving diffusion depend on tip radius:

$$\Delta X = \Delta X_0 \left(1 - \frac{r^*}{r}\right) \quad \text{where} \quad \begin{aligned} \Delta X &= X_0 - X_r \\ \Delta X_0 &= X_0 - X_e \end{aligned}$$

Length rate of precipitate growth:

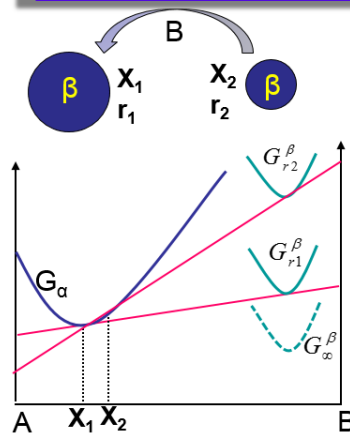
$$v = \frac{D \Delta X_0}{k(X_\beta - X_r)} \frac{1}{r} \left(1 - \frac{r^*}{r}\right)$$

- applies for volume diffusion control when supersaturation is kept constant;
- constant rate \rightarrow linear growth - $x \propto t$;
- applies also for growth of needle-shaped precipitate;
- faceted edges \rightarrow slower growth by ledge mechanism.

b) Describe Gibbs-Thomson effect and sketch Gibbs energy curves for precipitates of different shape/size. Based on it define Osterwald ripening. Give an example how fine precipitates can be stabilized in steel matrix. Presentation of the relevant equations as well as motivation of the answer are necessary to get full credit. (3 p)

Answer:

Particle Coarsening



High-density of fine precipitates tend to coarsen → decrease interfacial area → Ostwald ripening; Gibbs-Thomson effect: solute concentration in the matrix increases with particle size decreasing: $X_1 < X_2$; concentration gradient → solute diffuse to larger precipitates → coarsening of large precipitates; result: total number of particles decrease as the mean radius increases with time:

Assuming volume diffusion is rate controlling, it was shown:

$$\bar{r}^3 - r_0^3 = kt$$

$$k \propto D\gamma X_e$$

- $r=r_0$ at $t=0$;
- X_e – equilibrium solubility of very large particle.

D and X_e increase exponentially with T , coarsening rate:

$$\frac{d\bar{r}}{dt} \propto \frac{k}{\bar{r}^2}$$

Stabilization of fine precipitates:

Low γ : interfacial energy;

Stabilization of fine precipitates:

D : diffusion coefficient;

X_e : equilibrium solubility of $r=\infty$

- fully coherent precipitates;
- minimal misfit:
- **Nimonic** alloys: $\text{Ni}_3(\text{TiAl})$ (γ') – fully coherent with fcc Ni-matrix - good creep resist.

- strong carbide-formers – stabilize cementite due to much lower diffusion of substitutional elements;
- low-alloyed steels.

- oxides are very insoluble in metals – low X_e ;
- fine oxide dispersions in the matrix – high strength at high T ;
- W and Ni strengthened by ThO_2 .

c) Describe formation of the pearlite in the Fe-C alloys: nucleation, structure, orientation relationship to the primary austenitic grain, carbide morphology and precipitation, temperatures of formation, expressions for interlamellar spacing and transformation rate. Motivation of the answer is necessary to get full credit. (3p)

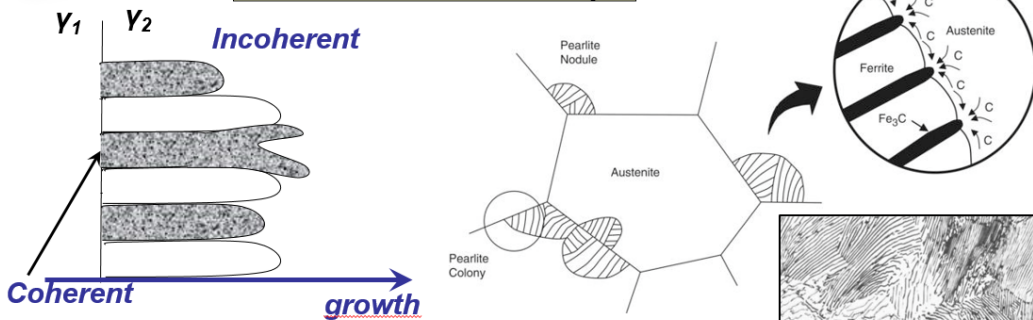
Answer: slides below

Ch:5.8. Eutectoid Transformations

Pearlite Reaction in Fe-C Alloys

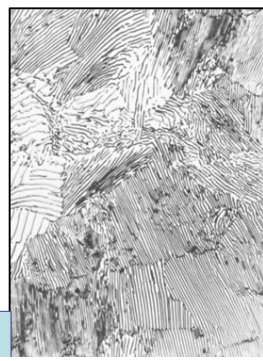
Similar to eutectic solidification:

In case of Fe-C: $\gamma \rightarrow \alpha + Fe_3C$



- nucleates on grain boundaries;
- coherent with one grain → orientational relationship, and incoherent with another;
- depleted solution around nuclei → driving force for nucleation of the second phase;
- Incoherent interface grow.

ASM Handbook - Volume 3, Alloy Phase Diagrams -> Solid-State Transformations -> Iron-Carbon Eutectoid Reaction



If alloy composition does not perfectly correspond to eutectic: some proeutectoid ferrite or cementite forms first:

- nuclei forms on the incoherent interface of allotriomorph with an orientational relationship;
- new lamellas forms as for eutectoid.

Interlamellar spacing and growth rate:

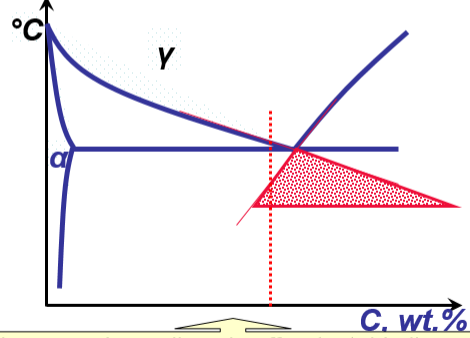
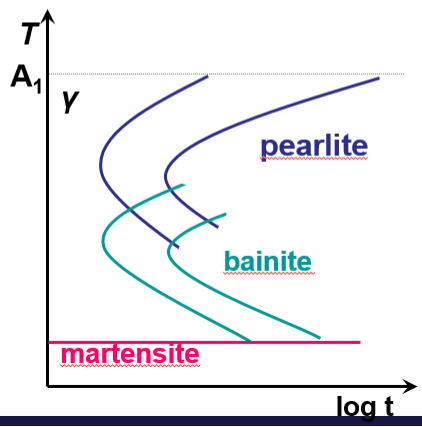
Pearlite Reaction in Fe-C Alloys

- The same treatment as growth of eutectic into the liquid:
- minimum spacing S^* , observed S_0 :
- the growth of pearlite colonies is controlled by C-diffusion in austenite:
- $k \rightarrow$ constant;
- diffusion through γ/α and γ/Fe_3C interface describes observed faster growth rates:
- maximum rate at $\sim 550^\circ C$, at lower temperatures \rightarrow bainite:

$$S_0 \propto S^* \propto \frac{1}{\Delta T}$$

$$v = kD_C^\gamma (\Delta T)^2$$

$$v = kD_b (\Delta T)^3$$



- larger undercoolings in off-eutectoid alloys
 → avoiding proeutectoid ferrite (risk for bainite though)

6. Diffusionless transformation (2 p)

Describe two types of martensite and effect of alloying elements on its nucleation/growth. Motivate your answer. (2p)

Austenite and ferrite stabilizing alloying elements – both lower transformation temperature:

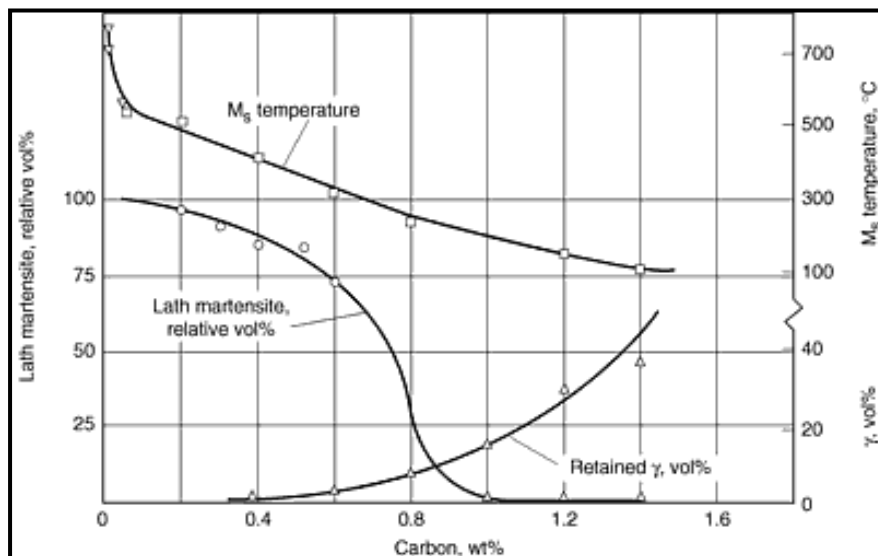
Andrews equation: $M_s(^{\circ}\text{C}) = 539 - 423(\text{C}) - 30.4(\text{Mn}) - 12.1(\text{Cr}) - 17.7(\text{Ni}) - 7.5(\text{Mo})$

Lath martensite - low carbon (0.4 wt.%C) low-alloyed steels:

- growth by nucleation dislocations at the highly-strained interface → misfit energy reduced and lath is able to continue growing;
- limited diffusion of carbon take place following/during transformation → connected to higher M_s temperature associated with lath martensite;
- low amount of residual austenite – sideway growth and transformation between laths is not probable to occur.

Plate martensite – medium and high carbon, high-nickel steels:

- associated with lower M_s and higher amount of retained austenite;
- medium C or Ni martensite → plates with twinned central "midrib" with outer regions being free of twins;
- high C or Ni martensite is completely twinned;
- growth mechanism is unclear.



7. Novel metallic materials (2 p)

Describe basic principles of formation of metallic glasses from thermodynamic point of view and their performance advantages in connection to their microstructure (2 p).

1. Alloys with ≥ 3 elements → "confusion principle" → atoms of significantly different sizes ($>12\%$) → high packing density and low free volume per atom → up to orders of magnitude higher viscosity than other metals and alloys in molten state → viscosity prevents the atoms moving enough to form an ordered lattice;
2. posses high entropy and should have negative heat of mixing → stabilization of glassy state → suppress crystal nucleation and prolongs the time the molten metal stays in supercooled state → no growth;
3. "deep" eutectics with low eutectic temperature → liquid state is stable

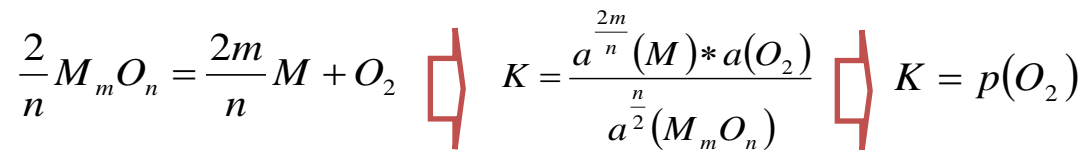
Advantages over conventional alloys:

1. absence of grain boundaries → better resistance to wear and corrosion;
2. are also much tougher and less brittle than oxide glasses and ceramics;
3. good electrical conductivity, high yield strength, high hardness, superior strength/weight ratio, superior elastic limit, high corrosion resistance, high wear-resistance, unique acoustical properties, etc.

8. Solid/gas interactions (2 p)

Estimate partial pressure of oxygen, required for dissociation of Fe_2O_3 at $T = 1000^\circ\text{C}$ if $\Delta G = 329.111 \text{ kJ}$. (ΔG is calculated for 1 mole O_2 according to the reaction $\frac{2}{n}M_mO_n = \frac{2m}{n}M + \text{O}_2$).

Answer:



$$\Delta G^0 = -RT \ln K \quad \Rightarrow \quad p(\text{O}_2) = \exp\left(-\frac{\Delta G_1^0}{RT}\right)$$

$$p(\text{O}_2)_{\text{Fe}_2\text{O}_3} = 3.134 \times 10^{-14} \text{ (bar)}$$